



Full paper/Mémoire

Zirconia-supported Keggin phosphomolybdovanadate nanocomposite: A heterogeneous and reusable catalyst for alkene epoxidation under thermal and ultrasonic irradiation conditions

Hossein Salavati^{a,*}, Shahram Tangestaninejad^b, Majid Moghadam^b, Valiollah Mirkhani^b, Iraj Mohammadpoor-Baltork^b

^a Department of Chemistry, Payame Noor University (PNU), Tehran 19395-4697, Islamic Republic of Iran

^b Department of Chemistry, Catalysis Division, University of Isfahan, Isfahan 81746-73441, Islamic Republic of Iran

ARTICLE INFO

Article history:

Received 25 February 2010

Accepted after revision 14 March 2011

Available online 12 May 2011

Keywords:

Phosphomolybdovanadate

Ultrasonic irradiation

Zirconia

Nanocomposite

Epoxidation

ABSTRACT

Keggin phosphomolybdovanadate, PVMo, was supported on a zirconia matrix by the wet impregnation method. The phase and chemical structure, optical absorption, surface physicochemical properties and morphology of PVMo–ZrO₂ composite were studied by X-ray diffraction (XRD) technique, FT-IR and diffuse reflectance UV–vis spectroscopic (DR UV–vis) methods, and scanning electron microscopy (SEM), which indicated that the primary Keggin structure has remained intact after formation of the composite. Moreover, the obtained nanocomposite was used as an efficient catalyst of olefins under reflux and ultrasonic irradiation conditions. The catalyst was reused several times, without observable loss of activity and selectivity. Indeed, the catalytic activity of the PVMo–ZrO₂ was compared with pure Keggin phosphomolybdovanadate.

© 2011 Académie des sciences. Published by Elsevier Masson SAS. All rights reserved.

1. Introduction

Polyoxoanions, as transition metal–oxygen–anion clusters, have attracted a great interest as homogeneous catalysts because of their acid–base and redox properties. Therefore, it is important to understand their catalytic role in different chemical reactions in which they are employed. They exhibit great advantages because their catalytic properties can be tuned by changing the identity of charge–compensating counteractions, heteroatoms, and framework metal atoms [1,2].

For various reasons, such as higher efficiency, better accessibility of the active sites, the environmentally friendly nature and lower cost supporting of a catalyst on a support is currently favored. The support does not always play merely a mechanical role; it can also modify

the catalytic properties of the catalyst. Although explanation of the true role of the supports is not clear, however, it appears that the nature of the support and the amount of the deposit may influence the catalytic properties of supported catalysts [3–6]. The sites influence the catalytic activity and selectivity of the catalysts in the epoxidation reactions. In recent years, zirconia has attracted much attention both as a catalyst and catalyst support because of its high thermal stability, amphoteric character and oxidizing and reducing properties [7–13].

Polyoxometalates can be used either directly as a bulk material or in supported form. The supported form is preferable because of its high surface area compared with the bulk material (5–8 m² g^{−1}) and better accessibility of reactants to the active sites. Owing to very low surface area and high solubility of these compounds in polar solvents, the development of supported and heterogeneously active forms of POM catalysts is in demand. POMs have been supported on different inorganic solids such as silica, mesoporous molecular sieve MCM-41 or MCM-48, NaY

* Corresponding author.

E-mail address: hosseinsalavati@pnu.ac.ir (H. Salavati).

zeolite, activated carbons, layered double hydroxide, amorphous or anatase TiO₂, montmorillonite and carbon nanotubes [14–37].

The main effect of ultrasound in liquids is cavitation phenomenon, which produces numerous tiny gas bubbles called cavitation bubbles. The collapse of these bubbles generates high temperatures and pressures are generated at the centre of the bubbles. These local effects produce a variety of radicals and highly active intermediates, which initiate other secondary chemical reactions in the bulk liquid. These radicals can react with contaminants to form by products.

The most successful applications of ultrasound have been found in the field of heterogeneous chemistry involving solids and metals. This is due to the mechanical impact of ultrasound on solid surfaces. In conventional chemistry there are several problems associated with reactions involving solids or metals: small surface area of the solid/metal may lead to excessive reactivity, penetration of reactants into deeper areas is not possible, oxide layers or impurities can cover the surface, reactants/products have to diffuse onto and from the surface and reaction products can act as deposit on the surface and prevent further reactions. The mechanical effects of ultrasound offer an opportunity to overcome the following types of problem associated with conventional solid/metal reactions: break-up of the surface structure allows penetration of reactants and/or release of materials from the surface, degradation of large solid particles due to shear forces induced by shock waves and microstreaming leads to reduction of particle size and increase of surface area and accelerated motion of suspended particles leads to better mass transfer [38].

Recently, we reported the sonocatalytic oxidation of organic compounds catalyzed by vanadium containing polyphosphomolybdate supported on MCM-41, TiO₂ nanoparticles, montmorillonite and carbon nanotubes [25,26]. In this paper, we wish to report the sonocatalytic oxidation of alkenes with H₂O₂ catalyzed by Na₅PV₂Mo₁₀O₄₀ (PVMo) supported on ZrO₂. The effect of ultrasonic irradiation on the catalytic activity of this catalyst was also investigated.

2. Experimental

All chemicals were of analytical grade and were used without further purification. Elemental analyses were performed on a Perkin-Elmer 2400 instrument. Atomic Absorption analyses were carried out on a Shimadzu 120 spectrophotometer. Compositional and elemental investigations were performed by backscattered electrons and EDX analysis, respectively. Diffuse reflectance spectra were recorded on a Shimadzu UV-265 instrument using optical grade BaSO₄ as reference. FT-IR spectra were obtained as potassium bromide pellets in the range 400–4000 cm⁻¹ with a Nicolet-Impact 400D instrument. Scanning electron micrographs of the catalyst and support were taken on SEM Philips XL 30. Powder X-ray diffraction data were obtained on a D₈ Advanced Bruker using Cu K α radiation (25–70°). Gas chromatography experiments (GC)

were performed on a Shimadzu GC-16A instrument using a 2 m column packed with silicon DC-200 or Carbowax 20 m. In all experiments, *n*-decane was used as internal standard. ¹H NMR spectra were recorded on a Bruker-Avance AQS 300 MHz using CDCl₃ as solvent and TMS as an internal reference. Conversions and yields were obtained by GC experiments and the products were identified after isolation and purification.

2.1. Preparation and characterization of PVMo–ZrO₂ composite

The Na₅[PV₂Mo₁₀O₄₀].14H₂O (PVMo) was prepared as described in the literature [39]. The typical procedure for preparation of PVMo–ZrO₂ nanoparticles is as following: PVMo (0.1 g) and ZrO₂ (0.4 g) were mixed and put into an agate mortar. The mixture was thoroughly ground for 20 min, washed in a supersonic washing machine using absolute alcohol as dispersant, and centrifuged. The washing and centrifuging processes were repeated five times. The wet nanoparticles of PVMo–ZrO₂ were obtained and dried in vacuum for 5 h (60–80 °C).

2.2. General procedure for oxidation reactions with H₂O₂ under reflux conditions

All reactions were carried out in a 50 mL thermostated glass reactor equipped with a magnetic stirrer. Temperatures were controlled with an accuracy of ± 2 K. In a typical experiment, the reaction vessel was loaded with the supported catalyst (containing 2.86 μ mol of PVMo), alkene (1 mmol) in acetonitrile (5 mL) and H₂O₂ (1 mL, 30%), and the mixture was refluxed. The progress of the reaction was monitored by GC. At the end of the reaction, the mixture was diluted with Et₂O (20 mL) and filtered. The catalyst was thoroughly washed with Et₂O and combined washings and filtrates were purified on a silica gel plate or a silica gel column. IR and ¹HNMR spectral data confirmed the identities of the products.

2.3. General procedure for oxidation reactions with H₂O₂ under ultrasonic irradiation

A UP 400S ultrasonic processor equipped with a 3 mm wide and 140 mm long probe, which was immersed directly into the reaction mixture, was used for sonication. The operating frequency was 24 kHz and the output power was 0–400 W through manual adjustment. The final volume of solution was 6 mL. The temperature of the solution reached 60 °C during sonication.

To a mixture of alkene (1 mmol) and the supported catalyst (containing 2.86 μ mol of PVMo) in acetonitrile (5 mL) was added hydrogen peroxide (1 mL, 30%) and the mixture was exposed to ultrasonic irradiation. The reaction progress was monitored by GC. After the reaction was completed, the reaction mixture was diluted with Et₂O (20 mL) and filtered. The catalyst was thoroughly washed with Et₂O and combined washings and filtrates were purified on a silica gel plates or a silica gel column. IR and ¹HNMR spectral data confirmed the identities of the products.

3. Results and discussion

3.1. Preparation and characterization of PVMo–ZrO₂ composite

Since phosphomolybdo vanadate of the Keggin structure have molecular diameters of ~ 12 Å, it is feasible to support phosphomolybdo vanadate on ZrO₂. The XRD patterns of zirconia and the PVMo–ZrO₂ composite are shown in Fig. 1A and B, respectively. In the XRD of ZrO₂, the diffraction peaks at $2\theta = 28.6^\circ$, 31.5° , 34.5° , 50.5° and 60.1° correspond to the tetragonal zirconia phase. Fig. 1B shows that the Keggin unit has been dispersed homogeneously into the ZrO₂ framework. The sizes of these nanoparticles, calculated from the data of XRD peak broadening according to the Scherer equation: $D = 0.89\lambda/\beta\cos\theta$ [40,41], was obtained as 35 nm.

Fig. 2 shows SEM images of nanoparticles. The morphologies and microstructure of the nanoparticles are approximately spherical. It is well-known that the catalytic activity of composites is strongly dependent on the shape, size and size distribution of the particles. Therefore, it is important to characterize the microstructure of the composite. Fig. 2b shows the SEM images of the PVMo–ZrO₂ powder. SEM image reveals that the powder is composed of aggregated fine particles and the average particle sizes is about 40 nm which is consistent with the

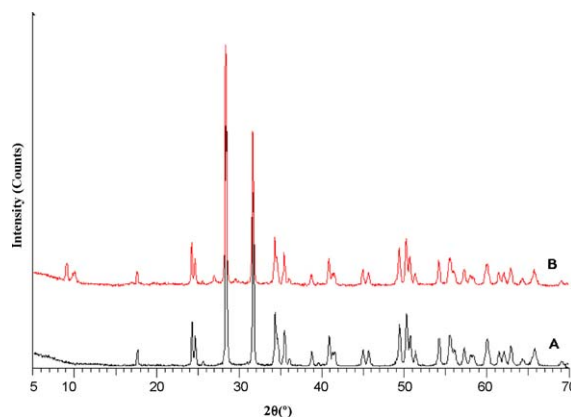


Fig. 1. XRD patterns of: (A) ZrO₂ (B) PVMo–ZrO₂ nanocomposite.

average size obtained from the peak broadening in X-ray diffraction studies.

FT-IR spectrum of the prepared catalyst showed absorption bands at 1072, 959, 866 and 787 cm⁻¹, corresponding to the four typical skeletal vibrations of the Keggin polyoxoanions, which indicated that PVMo has been supported on zirconia (Fig. 3). These peaks could be attributed to $\nu(P=O_a)$, $\nu(Mo=O_t)$, $\nu(Mo-O_b-Mo)$ and $\nu(Mo-O_c-Mo)$, respectively (O_t = terminal oxygen, O_b = bridged

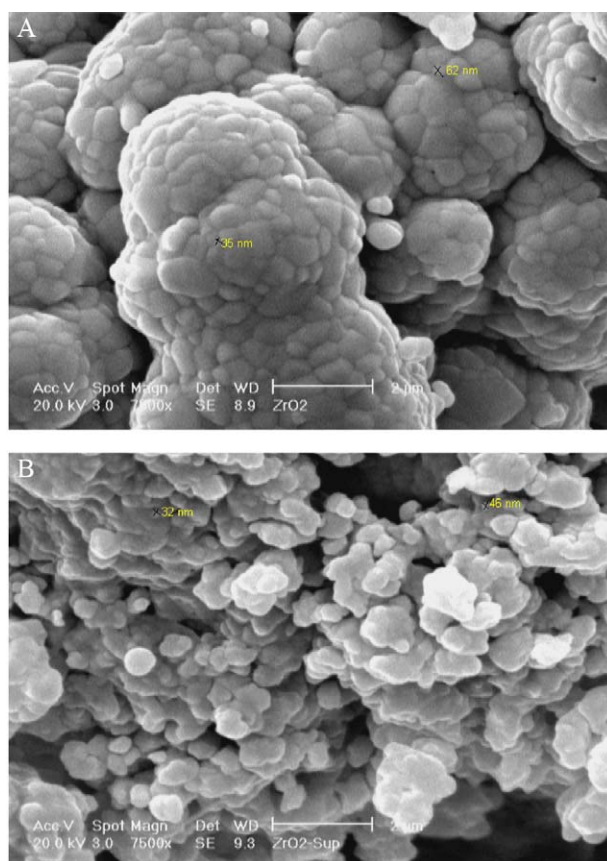


Fig. 2. SEM images of: (A) ZrO₂ and (B) PVMo–ZrO₂ nanocomposite.

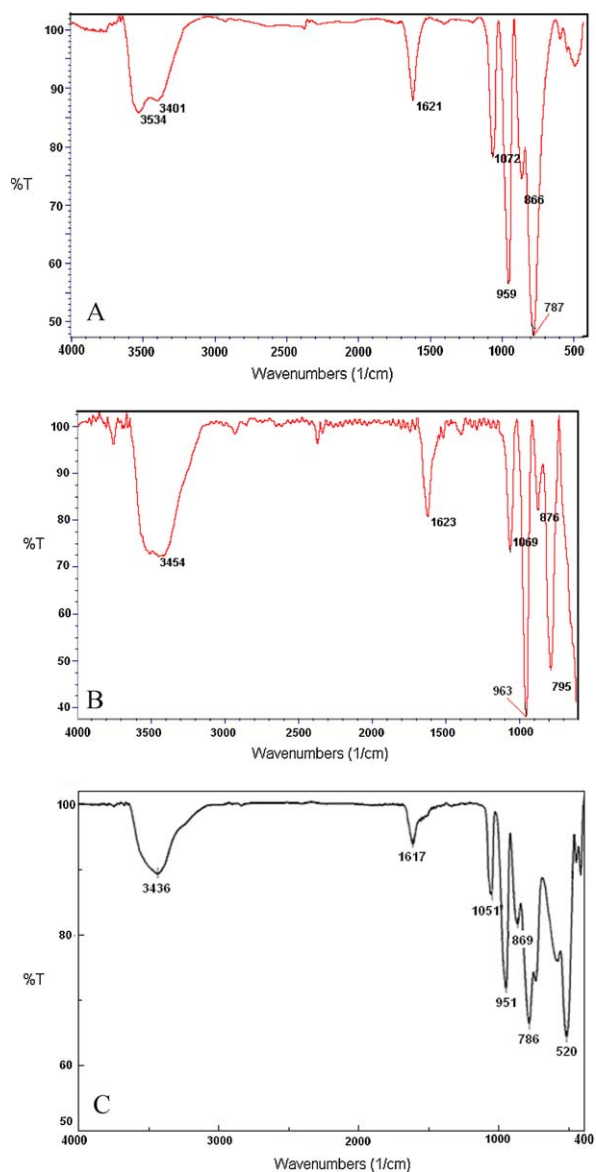


Fig. 3. FT-IR spectra of: (A) PVMo; (B) PVMo-ZrO₂, and (C) Recovered PVMo-ZrO₂ nanocomposite.

oxygen of two octahedral sharing a corner and O_c = bridged oxygen sharing an edge). The IR spectra indicated that the structure of the polyoxoanion has been retained upon impregnation. Therefore, it is confirmed that a strong chemical interaction, not simple physical absorption, exists between the polyanion and the zirconia surface. The broad and strong band at about 600 cm⁻¹ is attributed to the Zr–O stretching vibration of tetragonal ZrO₂ [42–45].

The UV-Vis spectra of PVMo in CH₃CN displayed absorption peaks at 266 and 308 nm, which are associated with octahedrally coordinated Mo⁶⁺ and arise due to the Mo–O and V–O charge-transfer absorptions in the heteropoly cage. These two absorption peaks appeared in the solid-state UV-vis spectra of the catalyst, since pure ZrO₂ shows no UV absorption peak; therefore, these results indicated that primary Keggin structure has

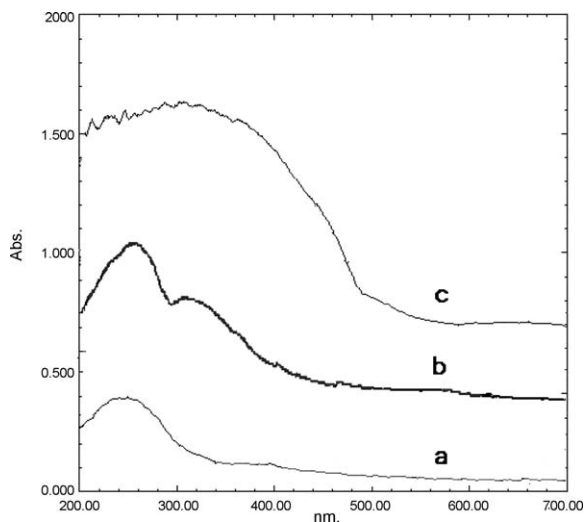


Fig. 4. UV-Vis DR spectra of: (a) ZrO₂ (b) PVMo, and (c) PVMo-ZrO₂ nanocomposite.

been introduced into the nanostructure framework (Fig. 4).

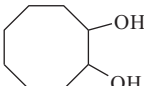
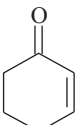
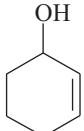
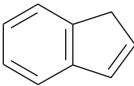
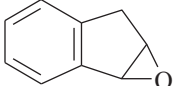
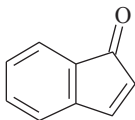
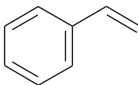
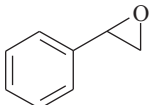
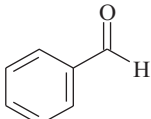
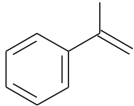
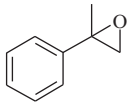
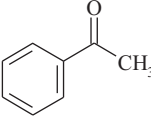
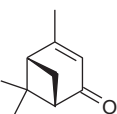
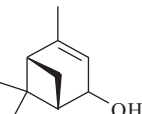
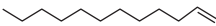
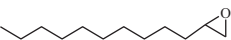
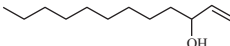
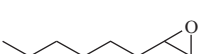
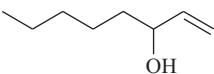
It is evident that the electronic spectrum of nanocomposite (Fig. 4c), with a broad and strong absorption peak in 200–400 nm, is different from pure ZrO₂ (Fig. 4a) and pure PVMo (Fig. 4b). As shown in Fig. 4, after formation of PVMo-ZrO₂ nanocomposite, the O→Mo charge transfer peak of PVMo (266 nm) and O→Zr charge transfer peak of ZrO₂ (247 nm) disappear, and a broad absorption peak appears.

The PVMo-ZrO₂ nanocomposite containing 20 wt% of POM was prepared through entrapment of catalyst into zirconia matrix via the wet impregnation method. (The ratio of PVMo to ZrO₂ was also checked by elemental analysis of the supported catalyst. In this manner, the amounts of Mo and Zr were determined by Neutron Activation Analysis. The obtained results confirmed that the amount of PVMo is about 20 wt%). In this process, POM-ZrO₂ nanocomposite is formed via electrostatic interaction and hydrogen bonding. This interaction also exists in H₃PW₁₂O₄₀-SiO₂ and H₄SiW₁₂O₄₀-SiO₂ composites; their preparation has been reported previously [36]. The hydrogen bonding is formed in the nanocomposite between the oxygen atoms of the PVMo and the ≡Zr–OH groups of the zirconia network, which can be expressed in the forms of Mo=O_t...HO–Zr≡ and Mo–O_b...HO–Zr≡, where O_t and O_b refer to the terminal and the bridge oxygen atoms in the PVMo unit, respectively. These two interactions confirm the fixation of the Keggin unit into the ZrO₂ support firmly, so that the leaching of PVMo in liquid phase reactions may be decreased [46,47].

3.2. Catalytic activity

Since heterogeneous catalysts are recoverable, hence, heterogenization of homogenous catalysts is of great interest. Therefore, we decided to immobilize PVMo on zirconia nanoparticles, and investigate its catalytic activity in the epoxidation of alkenes with H₂O₂ under agitation with magnetic stirring (MS) and under ultrasonic irradiation (US).

Table 1
Epoxidation of olefins with H₂O₂ catalyzed by PVMo–ZrO₂ under reflux conditions.^a

Entry	Substrate	Products	Time (h)	Conversion (%) ^{b,c}	Epoxide Selectivity (%) ^b	TOF (h ⁻¹)
1		 	10	70	80	24.5
2		  	10	65	73	22.7
3		 	10	48	59	16.8
4		 	10	90	85 ^d	31.5
5		 	10	88	85 ^e	30.8
6		  	10	45	42 ^f	15.8
7		 	10	28	45 ^g	9.8
8		 	10	58	46 ^h	20.3

^a Reaction conditions: olefin (1 mmol), catalyst (2.86 μmol), H₂O₂ (1 mL), CH₃CN (5 mL).

^b Based on the starting olefin.

^c GC yield.

^d 13.5% benzaldehyde was produced.

^e 13% acetophenone was detected as by product.

^f 16% verbenone and 10% verbenol were produced.

^g 12% alcohol was produced.

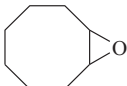
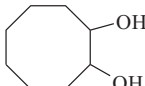
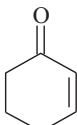
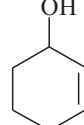
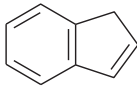
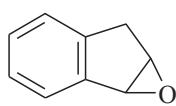
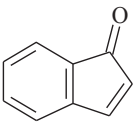
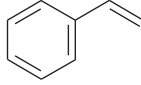
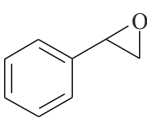
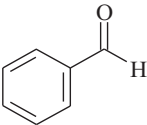
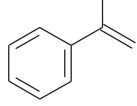
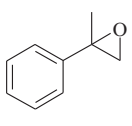
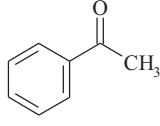
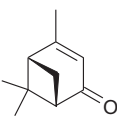
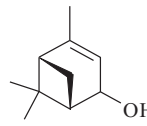
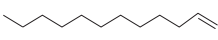
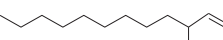
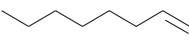
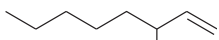
^h 31% alcohol was detected.

3.2.1. Alkene epoxidation with H₂O₂ catalyzed by PVMo–ZrO₂ under reflux conditions

First, the ability of the prepared catalyst, PVMo–ZrO₂, was investigated in the epoxidation of cyclooctene with H₂O₂ in acetonitrile. The reactions were continued until no

further progress was observed (Table 1). The results showed that the conversion was 70% with 80% epoxide selectivity. Epoxidation of cyclohexene showed 65% conversion and the epoxide selectivity was 73%, and allylic oxidation products (cyclohexene-1-one and cyclohexene-

Table 2
Epoxidation of olefins with H₂O₂ catalyzed by PVMo–ZrO₂ under ultrasonic irradiation.^a

Entry	Substrate	Products	Time (min)	Conversion (%) ^{b,c}	Epoxide Selectivity (%) ^b	TOF (h ⁻¹)
1		 	40	93	97	493
2		  	40	100	98	530
3		 	40	75	78	397
4		 	40	100	90 ^d	530
5		 	40	100	89 ^e	530
6		  	40	80	75 ^f	424
7		 	40	50	58 ^g	265
8		 	40	85	82 ^h	450

^a Reaction conditions: olefin (1 mmol), catalyst (2.86 μmol), H₂O₂ (1 mL), CH₃CN (5 mL).

^b Based on the starting olefin.

^c GC yield.

^d 10% benzaldehyde was produced.

^e 11% acetophenone was detected as by product.

^f 20% verbenone and 11% verbenol were produced.

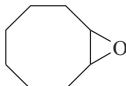
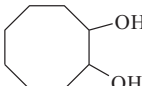
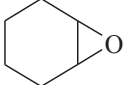
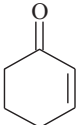
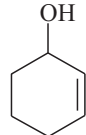
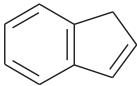
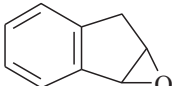
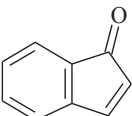
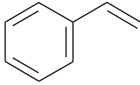
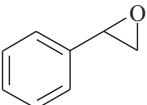
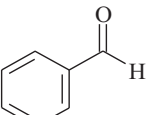
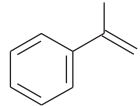
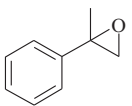
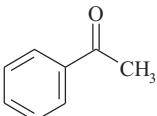
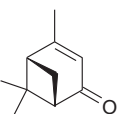
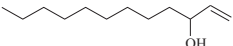
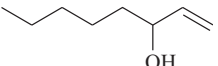
^g 21% alcohol was produced.

^h 15% alcohol was detected.

1-ol) were detected in the reaction mixture. In the case of indene, styrene and α-methyl styrene, the corresponding epoxides were obtained in 48, 90 and 88% epoxide selectivity. In the oxidation of α-pinene, the major product was α-pinene oxide, while verbenone and verbenol were

produced as minor products. Oxidation of linear alkenes such as 1-octene and 1-dodecene was accompanied by allylic oxidation. A blank experiment in the absence of the catalyst showed only small amounts of products in the oxidation of cyclooctene with H₂O₂.

Table 3
Epoxidation of olefins with H₂O₂ (30%) catalyzed by homogeneous PVMo under reflux conditions.^a

Entry	Substrate	Products	Time (h)	Conversion (%) ^{b,c}	Epoxide Selectivity (%) ^b	TOF (h ⁻¹)
1		 	20	55	95	9.6
2		  	20	44	85	7.7
3		 	20	35	49	6.1
4		 	20	43	29	7.5
5		 	20	27	42	4.7
6		  	20	20	52	3.3
7		 	20	26	58	4.5
8		 	20	30	31	5.2

^a Reaction conditions: olefin (1 mmol), catalyst (2.86 μmol), H₂O₂ (1 mL), CH₃CN (5 mL).

^b GC yield based on the starting olefin.

3.2.2. Alkene epoxidation with H₂O₂ catalyzed by PVMo–ZrO₂ under ultrasonic irradiation

As mentioned in the previous works, ultrasonic irradiation can be used as an efficient tool to influence the product yield and selectivity [10,11]. Therefore, we decided to investigate the effect of ultrasonic waves on the epoxidation of different alkenes with H₂O₂ catalyzed by PVMo–ZrO₂. As shown in Table 2, application of ultrasonic waves in this catalytic system has reduced the reaction

times and improved the yields and products selectivities. The system under ultrasonic irradiation showed a good catalytic activity in the oxidation of linear alkenes such as 1-octene and 1-dodecene.

The power of ultrasound is a very important parameter and also has a great influence on the phenomena of acoustic cavitation and efficiency of ultrasound treatment. Fig. 5 shows the effect of irradiation power on the epoxidation of cyclooctene, which indicates that increas-

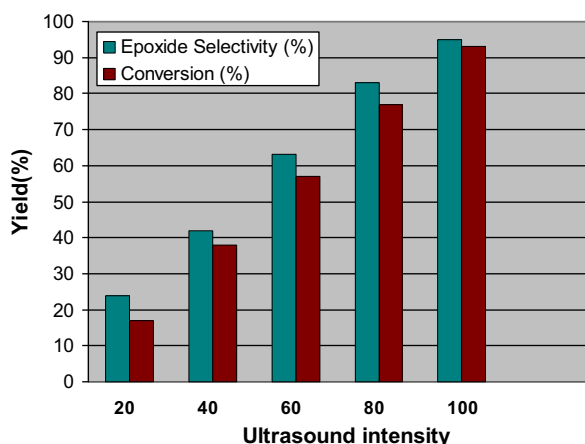


Fig. 5. The effect of ultrasonic irradiation intensity on the oxidation of cyclooctene with H_2O_2 catalyzed by PVMO-ZrO_2 .

ing of ultrasound power will improve the extent of oxidation and the highest conversion, was observed at a power of 400 W.

Fig. 6 comprises systems under ultrasonic irradiation and under agitation with magnetic stirring, which indicates that the catalytic activity of PVMO-ZrO_2 catalyst has been enhanced by ultrasonic irradiation.

The blank experiments in the absence of catalyst showed that ultrasonic irradiation has poor ability to epoxidize the alkenes with hydrogen peroxide.

In order to show the effect of ultrasonic irradiation on the catalytic activity enhancement, the particle size distribution of the catalysts was determined before and after sonication. The results showed that the catalyst agglomerates break-up during the sonication process. It seems that a part of ultrasonic irradiation effect is due to this phenomenon. To stress this point, the catalytic activity of a sonicated sample catalyst was studied in the epoxidation of cyclooctene under conventional mechanical stirring. It was found that the reaction time reduced from 10 h to 6.5 h for epoxidation of cyclooctene. These results show that in addition to break-up of the agglomerates, other factors such as thorough mixing of the reactants and producing of hot spots are the main reasons for catalytic enhancement by ultrasonic irradiation. On the other hand, collapse of the produced bubbles results in generation of high temperatures. As the reaction under mechanical stirring requires a temperature of about 80°C , therefore,

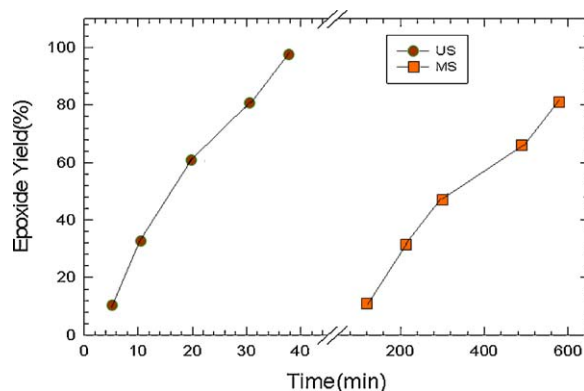


Fig. 6. Comparison of Ultrasonic irradiation and magnetic agitation in the oxidation of cyclooctene with H_2O_2 catalyzed by PVMO-ZrO_2 .

the reaction can be also accelerated under ultrasonic irradiation.

In order to show the effect of support on the catalytic activity, all reactions were repeated in the presence of homogeneous PVMO catalyst and under the same reaction conditions. It is clear from Tables 1 and 3 that the catalytic activity of PVMO-ZrO_2 was much higher than that of unsupported heteropolyanion. The conversions, selectivities and TOFs are higher for heterogeneous PVMO-ZrO_2 in comparison with the homogeneous one. Therefore, the catalytic activity increases by dispersing of the catalyst on the ZrO_2 . On the other hand, the ability of ZrO_2 , as catalyst, was checked in the oxidation of cyclooctene with H_2O_2 . The obtained results showed that ZrO_2 has poor ability to catalyze the epoxidation of cyclooctene and the amount of epoxide was less than 3%.

3.2.3. Catalyst reuse and stability

The stability of the supported catalyst was monitored using multiple sequential oxidation of cyclooctene with hydrogen peroxide under reflux or ultrasonic irradiation. For each of the repeated reactions, the catalyst was recovered, washed thoroughly with acetonitrile and 1,2-dichloroethane, successively, and dried before being used with fresh cyclooctene and hydrogen peroxide. In both cases, the catalysts were consecutively reused four consecutive times (Table 4). Addition of fresh alkene and oxidant to the filtrates showed that the amount of epoxide is comparable to the blank experiments. These results are in accordance with the leaching data. The nature of the

Table 4

The results obtained from catalyst reuse and stability in the oxidation of cyclooctene with magnetic stirring (MS) and under ultrasonic irradiation (US).^a

Run	Time		Conversion (%) ^b		Epoxide Selectivity (%)		V leaching (%) ^c	
	MS (h)	US (min)	MS	US	MS	US	MS	US
1	10	40	70	93	80	97	1.0	1.0
2	10	40	68	92	80	97	0.8	0.7
3	10	40	68	91	80	97	0.4	0.5
4	10	40	68	90	80	97	0.0	0.0

^a Reaction conditions: olefin (1 mmol), catalyst (2.86 μmol), H_2O_2 (1 mL), CH_3CN (10 mL).

^b GC yield based on the starting olefin.

^c Determined by ICP.

recovered catalyst was followed by IR. After reusing the catalyst for several times, no change in the IR spectra was observed (Fig. 3 C).

4. Conclusions

Supporting of phosphomolybdo vanadate on nanoparticle materials such as ZrO₂ gave a catalyst, which was recoverable and reusable in the oxidation of alkenes with hydrogen peroxide. The use of ultrasonic irradiation increased the conversions and reduced the reaction times. The results showed that good catalytic activity of the heteropolymolybdate, especially under ultrasonic irradiation; make them as useful catalysts for further applications in the area of catalysis. We have directly observed the attachment of PVMos nanoparticles to ZrO₂ due to the chemical adsorption between hydroxyl groups of ZrO₂ and PVMo nanoparticles.

Acknowledgement

The support of this work by Payame Noor University (PNU) and Catalysis Division of University of Isfahan (CDUE) is acknowledged.

References

- [1] B. Keita, L. Nadjo, *J. Mol. Catal. A: Chem* 262 (2007) 190.
- [2] L.R. Pizzio, P.G. Vazquez, C.V. Caceres, M.N. Blanco, *Appl. Catal. A: Gen* 256 (2003) 125.
- [3] M. Fournier, R. Thouvenot, C.R. Deltcheff, *J. Chem. Soc. Faraday Trans* 87 (1991) 349.
- [4] N. Mizuno, K. Yamaguchi, K. Kamata, *Coord. Chem. Rev* 249 (2005) 1944.
- [5] G. Suss-Fink, L. Gonzalez, G.B. Shalpin, *Appl. Catal. A: Gen* 217 (2001) 111.
- [6] Y. Guo, C. Hu, X. Wang, E. Wang, Y. Zhou, S. Feng, *Chem. Mater* 13 (2001) 4058.
- [7] X. Qu, Y. Guo, C. Hu, *J. Mol. Catal. A: Chem* 262 (2007) 128.
- [8] J.L. Capelo, C. Maduro, C. Vilhena, *Ultrason. Sonochem* 12 (2005) 225.
- [9] N.J. Miller-Ihli, *Fresenius J. Anal. Chem* 345 (1993) 482.
- [10] N.D. Rassokhin, V.K. Georgii, T.L. Bugaenko, *J. Am. Chem. Soc* 117 (1995) 344.
- [11] B. Devassy, F. Lefebvre, W. Bohringer, J. Fletcher, S.B. Halligudi, *J. Mol. Catal. A: Chem* 236 (2005) 162.
- [12] B. Devassy, F. Lefebvre, S.B. Halligudi, *J. Catal* 231 (2005) 1.
- [13] B.M. Devassy, S.B. Halligudi, S.G. Hegde, A.B. Halgeri, F. Lefebvre, *Chem. Commun.* (2002) 1074–1075.
- [14] Y. Wu, X. Ye, X. Yang, X. Wang, W. Chu, Y. Hu, *Ind. Eng. Chem. Res* 35 (1996) 2546.
- [15] O.A. Kholdeeva, R.I. Maksimovskaya, *J. Mol. Catal. A: Chem* 262 (2007) 7.
- [16] A. Molinari, R. Amadelli, L. Andreotti, A. Maldotti, *J. Chem. Soc. Dalton Trans.* (1999) 1203–1204.
- [17] R.R. Ozer, J.L. Ferry, *Environ. Sci. Technol* 35 (2001) 3242.
- [18] R.R. Ozer, J.L. Ferry, *J. Phys. Chem. B* 106 (2002) 4336.
- [19] Y. Guo, C. Hu, C. Jiang, Y. Yang, S. Jiang, X. Li, E. Wang, *J. Catal* 217 (2003) 141.
- [20] Y. Guo, C. Hu, S. Jiang, C. Guo, Y. Yang, E. Wang, *Appl. Catal. B: Environ* 36 (2002) 9.
- [21] Y. Yang, Y. Guo, C. Hu, Y. Wang, E. Wang, *Appl. Catal. A: Gen* 273 (2004) 201.
- [22] Y. Yang, Q. Wu, Y. Guo, C. Hu, E. Wang, *J. Mol. Catal. A: Chem* 225 (2005) 203.
- [23] S. Tangestaninejad, V. Mirkhani, M. Moghadam, I. Mohammadpoor-Baltork, E. Shams, H. Salavati, *Ultrason. Sonochem* 15 (2008) 438.
- [24] S. Tangestaninejad, M. Moghadam, V. Mirkhani, I. Mohammadpoor-Baltork, E. Shams, H. Salavati, *Catal. Commun* 9 (2008) 1001.
- [25] H. Salavati, S. Tangestaninejad, M. Moghadam, V. Mirkhani, I. Mohammadpoor-Baltork, *Ultrason. Sonochem* 17 (2010) 145.
- [26] H. Salavati, S. Tangestaninejad, M. Moghadam, V. Mirkhani, I. Mohammadpoor-Baltork, *Ultrason. Sonochem* 17 (2010) 453.
- [27] S. Damyanova, L. Dimitrov, R. Mariscal, J.L.G. Fierro, L. Petrov, I. Sobrados, *Appl. Catal. A: Gen* 256 (2003) 183.
- [28] M. Faraj, J.M. Brégeault, J. Martin, C. Martin, *J. Organomet. Chem* 276 (1984) c23.
- [29] J.M. Brégeault, C. Aubry, G. Chottard, N. Platzer, F. Chauveau, C. Huet, H. Ledon, *Stud. Surf. Sci. Catal* 66 (1991) 521.
- [30] J.M. Brégeault, B. El Ali, J. Mercier, J. Martin, C. Martin, O. Mohammedi, *Stud. Surf. Sci. Catal* 55 (1990) 205.
- [31] C. Minot, R. Thouvenot, J.Y. Piquemal, L. Salles, J.M. Brégeault, *J. Mol. Catal. A: Chem* 117 (1997) 375.
- [32] A.M. Khenkin, R. Neumann, A.B. Sorokin, A. Tuel, *Catal. Lett* 63 (1999) 189.
- [33] R. Neumann, A.M. Khenkin, *Chem. Commun.* (2006) 2529–2538.
- [34] M. Vasylyev, D.S. Rozner, A. Haimov, G. Maayan, R. Neumann, *Topics in Catal.* 34 (2005) 93.
- [35] M.V. Vasylyev, R. Neumann, *J. Am. Chem. Soc* 126 (2004) 884.
- [36] A.M. Khenkin, R. Neumann, *J. Am. Chem. Soc* 126 (2004) 6356.
- [37] G. Maayan, R. Neumann, *Chem. Commun.* (2005) 4595–4597.
- [38] T. Mason, D. Peters, *Practical Sonochemistry*, 2nd Ed., Horwood publishing Chichester, 2002., p. 17.
- [39] K. Nomiyama, S. Matsuoka, T. Hasegawa, Y. Nemoto, *J. Mol. Catal. A: Chem* 156 (2000) 143.
- [40] T. Ilkenhans, B. Herzog, T. Braun, R. Schlogl, *J. Catal* 153 (1995) 275.
- [41] B.R. Jermy, A. Pandurangan, *Appl. Catal. A: Gen* 295 (2005) 185.
- [42] M.A. Hamon, H. Hu, P. Bhowmik, S. Niyogi, B. Zhao, M.E. Itkis, R.C. Haddon, *Chem. Phys. Lett* 347 (2001) 8.
- [43] K. Nakamoto, *Infrared and Raman Spectra of Inorganic and Coordination Compounds*, 4th ed., Wiley, New York, 1986.
- [44] C. Rocciccioli-Deltcheff, M. Frank, R. Thouvenot, *Inorg. Chem* 22 (1983) 207.
- [45] A. Chemseddin, C. Sanchez, J. Livage, J. Launay, M. Fournier, *Inorg. Chem.* 23 (1984) 2609.
- [46] M. Valigi, D. Gazzoli, G. Ferraris, E. Bemporad, *Phys. Chem. Chem. Phys* 21 (2003) 4974.
- [47] J.B. Moffat, in: B. Imelik (Ed.), *Catalysis by Acids and Bases*, Elsevier, Amsterdam, 1985, p. 157.